iScience

CellPress
OPEN ACCESS

Article

Allograft inflammatory factor-1-like is a situational regulator of leptin levels, hyperphagia, and obesity

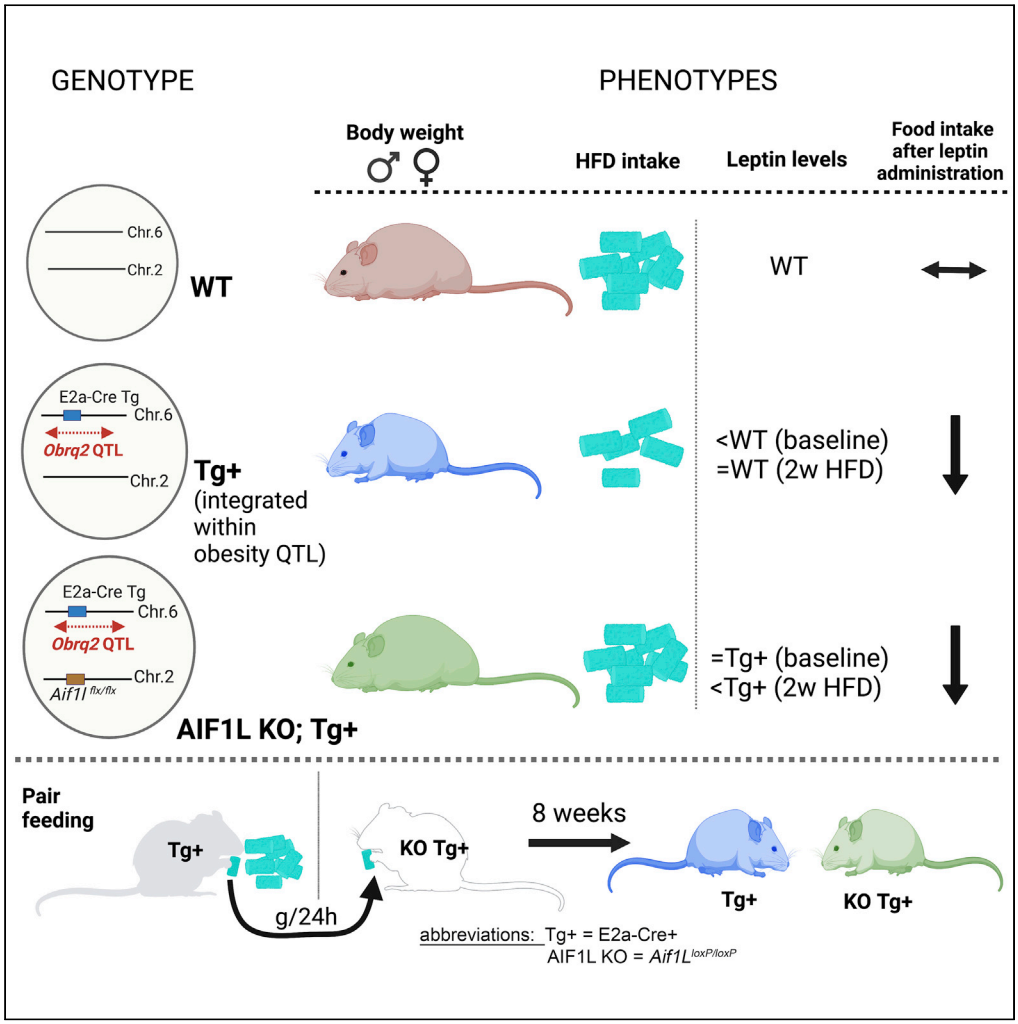

Dippal Parikh, Smitha Jayakumar, Gustavo H. Oliveira-Paula, Vanessa Almonte, Dario F. Riascos-Bernal, Nicholas E.S. Sibinga

nicholas.sibinga@einsteinmed.edu

Highlights

A widely used transgene—*E2a-Cre*—lies within an obesity QTL on mouse chromosome 6

E2a-Cre limits high-fat diet intake and weight gain, and increases leptin sensitivity

Obesity resistance conferred by the transgene is reversed by loss of AIF1L

AIF1L acts as a genetic modifier of the *Obrq2* obesity QTL and leptin levels

Parikh et al., iScience *25*, 105058
October 21, 2022
https://doi.org/10.1016/j.isci.2022.105058

iScience

CellPress
OPEN ACCESS

Article

Allograft inflammatory factor-1-like is a situational regulator of leptin levels, hyperphagia, and obesity

Dippal Parikh,[1] Smitha Jayakumar,[1] Gustavo H. Oliveira-Paula,[1] Vanessa Almonte,[1] Dario F. Riascos-Bernal,[1] and Nicholas E.S. Sibinga[1,2,*]

SUMMARY

Mouse models enable the study of genetic factors affecting the complex pathophysiology of metabolic disorders. Here, we identify reductions in leptin levels, food intake, and obesity due to high-fat diet, accompanied by increased leptin sensitivity, in mice that harbor the E2a-Cre transgene within *Obrq2*, an obesity quantitative trait locus (QTL) that includes the leptin gene. Interestingly, loss of allograft inflammatory factor-1-like (AIF1L) protein in these transgenic mice leads to similar leptin sensitivity, yet marked reversal of the obesity phenotype, with accelerated weight gain and increased food intake. Transgenic mice lacking AIF1L also have low circulating leptin, which suggests that benefits of enhanced leptin sensitivity are lost with further impairment of leptin expression due to loss of AIF1L. Together, our results identify AIF1L as a genetic modifier of *Obrq2* and leptin that affects leptin levels, food intake, and obesity during the metabolic stress imposed by HFD.

INTRODUCTION

Obesity is a major public health issue that affects staggering numbers of people, including adults and children alike. The interaction of genetic risk factors with our modern obesogenic environment contributes greatly to the rising incidence of this condition. Importantly, obesity is a major risk factor for a number of chronic diseases, including diabetes, cardiovascular disease, fatty liver disease, and several types of cancer (Hubert et al., 1983; Li et al., 2016; Colditz and Lindsay, 2018); in the current pandemic, it increases the risk of serious infection and death due to COVID-19 (Anderson et al., 2020; Tartof et al., 2020; Kompaniyets et al., 2021; Kuehn, 2021). Existing therapies for obesity include dietary regulation, weight loss surgery, and anti-obesity drugs, but the limited effectiveness, durability, and undesirable side effects of such approaches point to the need for better understanding of the pathophysiology of obesity that could lead to new therapeutic strategies and/or more effective dietary interventions.

Chromosome substitution strains (CSSs) provide a valuable tool to identify novel candidate genetic factors or modifier genes of known causal genes, regulating the pathophysiology of complex diseases such as obesity and its associated metabolic syndrome. A CSS in which chromosome 6 is derived from the A/J strain and the remainder of the genome is from the C57BL/6J strain shows resistance to diet-induced obesity (DIO) (Buchner et al., 2008). Further studies with congenic and sub-congenic strains of this CSS (B6.A6) revealed several obesity quantitative trait loci (QTLs) on chromosome 6, including *Obrq2*, which alone appears responsible for 50% of the body weight differences between the naturally DIO-resistant A/J strain and DIO-prone C57BL/6J strain (Buchner et al., 2008). So far, these QTLs discovered on chromosome 6 have helped to identify novel regulators of body weight, glucose homeostasis, and food intake (Yazbek et al., 2010, 2011; Buchner et al., 2012).

Obesity is characterized fundamentally by excessive accumulation of fat in adipose tissue due to an imbalance in energy intake and energy output. In addition to a central function in energy storage, adipose tissue is a critical endocrine organ, secreting hormones called adipokines. Leptin, the first adipokine identified, serves as an indicator of fat storage status throughout the body and acts as a critical regulator of energy intake. Congenital deficiency of leptin results in severe obesity in both rodents and humans (Montague et al., 1997). While null mutations of leptin and the leptin receptor are rare, individuals with heterozygous

[1]Department of Medicine (Cardiology), and Department of Developmental and Molecular Biology, Wilf Family Cardiovascular Research Institute, Albert Einstein College of Medicine, 1300 Morris Park Avenue, Bronx, NY 10461, USA

[2]Lead contact

*Correspondence: nicholas.sibinga@einsteinmed.edu

https://doi.org/10.1016/j.isci.2022.105058

mutations in the *leptin* gene also show increased body weight (Farooqi et al., 2001). Administration of exogenous leptin in the setting of leptin deficiency decreases food intake reduction and promotes weight loss (Farooqi et al., 1999) (Pelleymounter et al., 1995). Most obese subjects, however, have high levels of circulating leptin without a reduction in appetite, and do not eat less in response to exogenous leptin administration—a phenomenon called leptin resistance (Ogus et al., 2003; Gruzdeva et al., 2019).

Since the identification of leptin 25 years ago, its physiology has been studied extensively, but the basis of leptin resistance, especially under varied metabolic contexts, remains incomplete. A common aspect of several proposed mechanisms, however, is that hyperleptinemia is necessary to drive leptin resistance (Knight et al., 2010). Recent studies in mice suggest that a partial reduction in leptin levels can be beneficial in some settings (*e.g.*, high-fat diet) because these mice are protected from leptin resistance (Zhao et al., 2019, 2020). Overall, these observations put a much-needed spotlight on the definition and potential significance of "partial/low" leptin levels. Thus, studies identifying different factors that regulate leptin levels will help provide a more comprehensive view of its actions in physiological and pathophysiological conditions.

We previously reported that a protein called allograft inflammatory factor-1-like (AIF1L) is expressed in adipose tissues of mice and that AIF1L deficiency did not affect age-dependent weight gain or HFD-induced obesity. We also noted that loss of AIF1L reduced expression of *leptin* transcripts in adipose tissues and levels of leptin in the circulation (Parikh et al., 2020). In subsequent work, we have found that AIF1L can modify susceptibility to HFD-induced obesity in some settings. This observation arises from studies in a transgenic mouse model—the E2a-Cre transgenic mouse line, referred to hereafter as Cre+—that is widely used to induce germline excision of floxed alleles (Lakso et al., 1996).

Our studies show that compared to WT mice, Cre+ mice display limited food intake and weight gain on HFD. Interestingly, the E2a-Cre transgene maps to a previously characterized chromosome 6 obesity resistance locus, *Obrq2*, that includes the *leptin* gene (Buchner et al., 2008). The presence of the transgene limits leptin levels at baseline compared to WT; Cre+ mice on long-term HFD respond to exogenous leptin with decreased food intake, while WT mice show no effect. Importantly, Cre+ mice show increased response to exogenous leptin also after brief HFD feeding, when the bodyweights have not yet diverged. Cre+ mice that are also homozygous for the *loxP*-modified *Aif1l* allele (genotype $Aif1l^{loxP/loxP}$;E2a-Cre+, and referred to as $Aif1l^{flox}$;Cre+) maintain this higher leptin sensitivity but have lower leptin levels shortly after starting on HFD.

In contrast to this apparently mild effect on leptin levels, AIF1L deficiency fully reverses the limited weight gain phenotype of the Cre+ mouse—that is, on HFD, Cre+ mice eat less and weigh less, whereas $Aif1l^{flox}$;Cre+ mice eat more and become markedly obese. In pair-feeding studies, these differences in weight gain disappear, implicating differential food intake as the major driver of obesity in $Aif1l^{flox}$;Cre+ mice eating an HFD. Together, these findings suggest a genetic interaction between the *Aif1l* locus and the integrated E2a-Cre transgene chromosomal region that may depend at least in part on leptin physiology—including regulation of levels as well as sensitivity, but associated with significant effects on food intake and obesity.

RESULTS

Compared to WT mice, Cre+ mice show limited weight gain upon HFD feeding

In our studies with normal (chow) diet, we observed that Cre+ and WT mice have similar body weights at 8–10 weeks of age (Figure 1A); incidentally, we observed that the Cre+ mice gain less weight compared to WT mice when subjected to HFD feeding for 16 weeks (Figures 1B and 1C). To evaluate if there are energy intake differences at this time point, we housed the mice individually and found that Cre+ mice have reduced cumulative food intake compared to WT mice, as measured over 7 days (Figure 1D). The reduced weight gain observed for the HFD-fed Cre+ mice was due to reduced fat as well as lean mass as measured by Echo MRI (Figure 1E). At the end of the study, we harvested organs and found reduced inguinal subcutaneous adipose tissue (iSAT) and liver mass (Figure 1F). Overall, these results indicate that E2a-Cre transgene integration limits food intake and HFD-induced weight gain.

The E2a-Cre transgene is integrated in a recognized obesity quantitative trait locus (QTL) on chromosome 6 that includes the leptin gene

Jackson laboratories provides a rough estimate of the E2a-Cre transgene integration site using single nucleotide polymorphism (SNP) testing, but the precise chromosomal location has not been previously

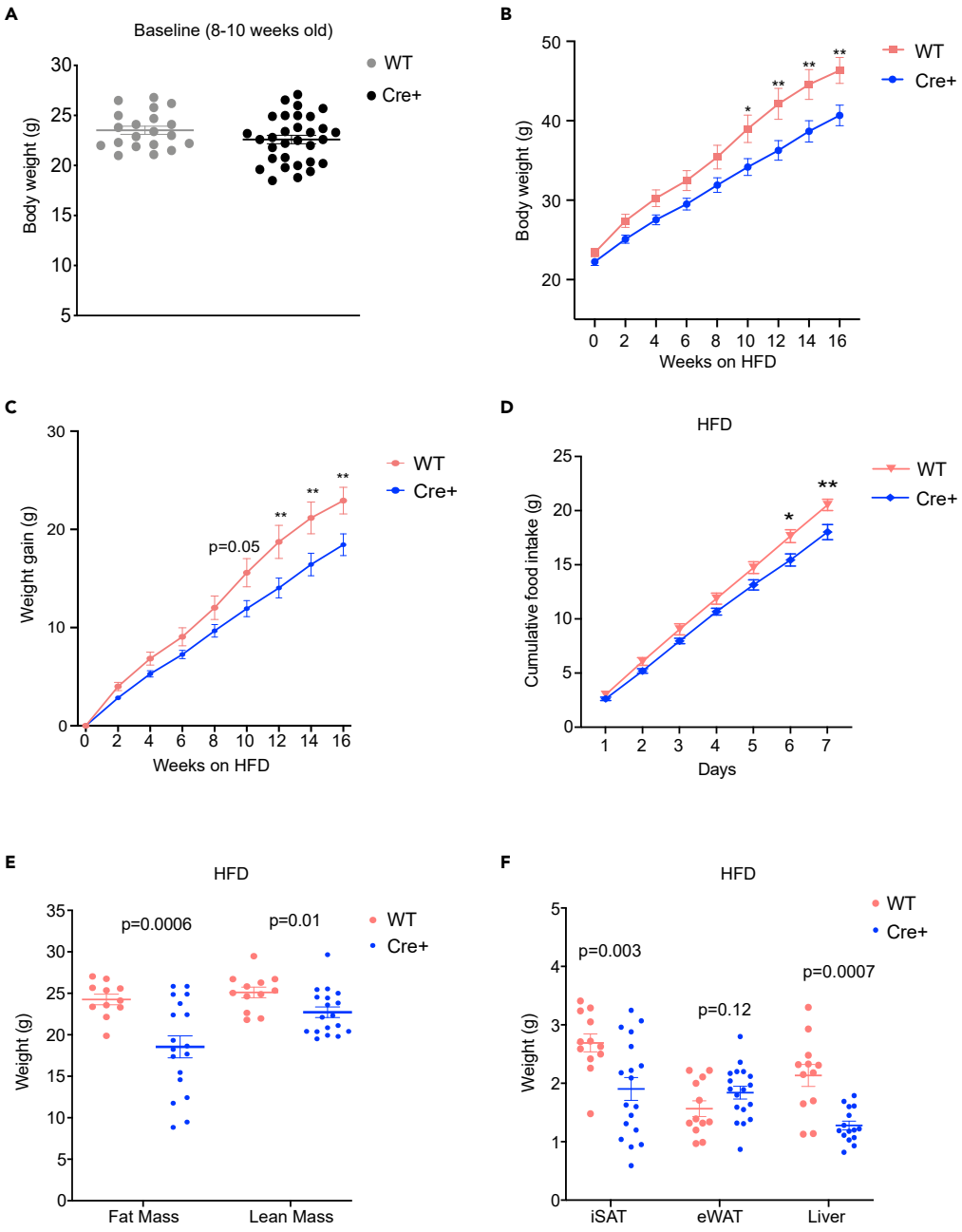

Figure 1. E2a-Cre transgenic mice show limited weight gain upon HFD feeding, compared to WT mice

(A) Body weight of 8–10 weeks old WT (n = 20) and E2a-Cre transgenic (Cre+) male mice (n = 31).

(B) Body weight curves of WT (n = 14) and Cre+ (n = 26) mice on high-fat diet for 16 weeks.

(C) Weight gain of WT (n = 14) and Cre+ (n = 26) male mice on high-fat diet for 16 weeks.

(D) Cumulative food intake of single housed male mice measured every 24 h for 7 days (WT; n = 6) (Cre+; n = 4).

(E) Fat mass and lean mass measurements of 16 weeks HFD-fed male mice, analyzed by Echo MRI (WT; n = 11–12) (Cre+; n = 18).

(F) Inguinal subcutaneous adipose tissue (iSAT), epididymal white adipose tissue (eWAT), and liver mass from 16 weeks HFD-fed male mice (WT; n = 12) (Cre+; n = 15–18). Data are represented as mean ± SEM.

reported. To determine the exact site—and possibly gain insight into how its integration affects metabolism—we used targeted locus amplification (TLA) to localize the transgene to chromosome 6 (Grcm38) at position 26,649,738 to 26,649,829 (Figures 2A and 2B). Transgene integration entails at least

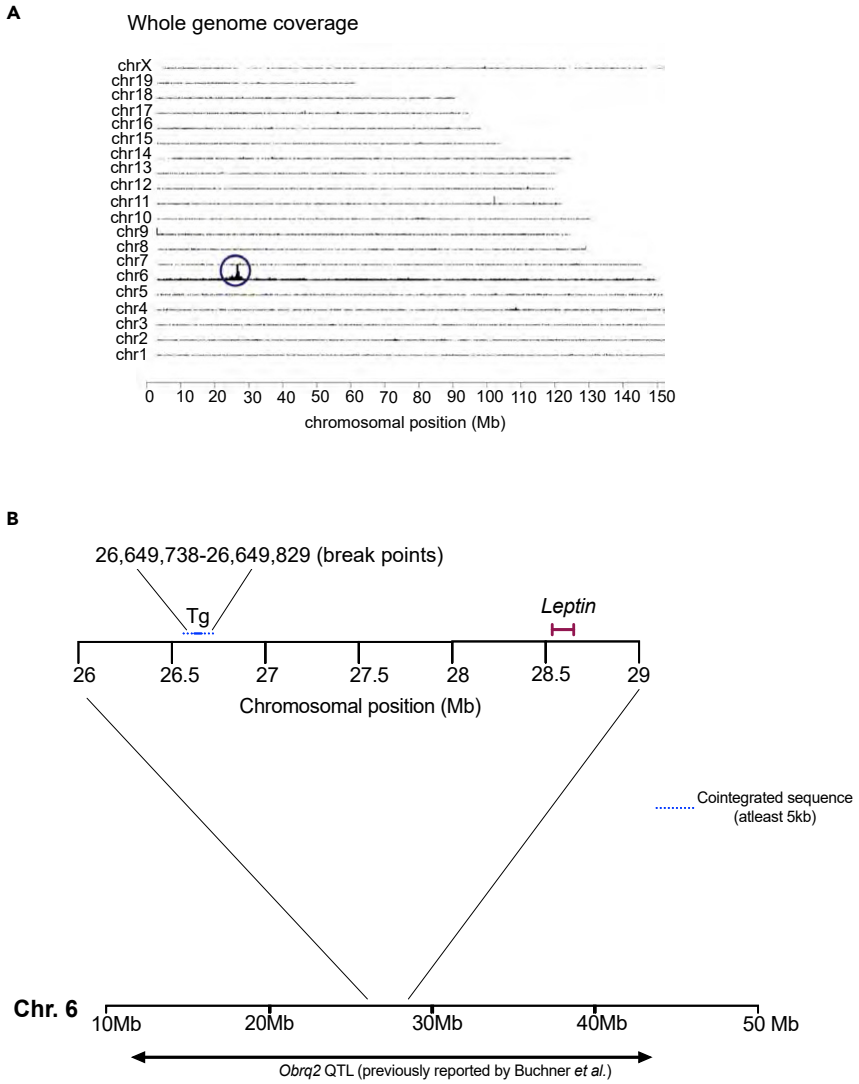

Figure 2. The E2a-Cre transgene is integrated in a recognized obesity quantitative trait locus (QTL) on chromosome 6 that includes the leptin gene

(A) Targeted locus amplification (TLA) sequence coverage across the mouse genome of the transgenic mice.

(B) Precise location and expanded chromosomal region of the transgene integration site.

5 kb of cointegrated sequence and a 91 bp genomic deletion; no concatemers (transgene-transgene fusions) were observed. This chromosomal location falls within a previously identified obesity quantitative trait locus (QTL) called *Obrq2* (Buchner et al., 2008; Yazbek et al., 2011). Importantly, *Obrq2* sequences are in synteny with regions on human chromosome 7 (7q21; 7q31-35) that have been shown to be associated with obesity. We observed with interest that this integration site is relatively close to the *leptin* gene (Figure 2B), but also noted prior linkage and linkage disequilibrium mapping analyses suggesting that at least two other genes within this interval influence obesity (Li et al., 2003).

Cre+ mice on HFD show higher responsiveness to exogenous leptin

We then assessed if the mutation of *Obrq2* induced by transgene insertion affects leptin expression. Since we found reduced food intake in long-term HFD-fed mice (Figure 1), we first checked leptin levels after 16 weeks of HFD feeding and noted a trend toward reduced levels of circulating leptin in Cre+ mice compared to WT mice (Figure 3A). Body composition analysis of this cohort of mice showed reduced fat mass of Cre+ mice compared to WT mice (Figure 3B). Plotting leptin levels as a function of fat mass did

not reveal any further differences (Figure S1). However, these curious results with Cre+ mice—showing reduced food intake, fat mass, and a trend toward lower absolute leptin levels relative to WT mice—led us to test leptin sensitivity at this time point in regard to its effect on food intake. The mice were housed singly and acclimatized for 1 week. To cover a range of doses, the leptin amount was escalated over days. Interestingly, when we measured food intake by these mice over a course of 7 days, we found that Cre+ mice responded to exogenous leptin administration with a reduction in food intake that was not observed in WT mice (Figure 3C). To determine if Cre+ mice have differential sensitivity to leptin even before the divergence in adiposity and body weight, we performed the same experiment in mice fed an HFD for just 2 weeks. We observed a pronounced decrease in cumulative food intake in Cre+ mice, while WT mice did not show a difference relative to PBS administration (Figure 3D). While leptin administration on day 1 reduced food intake similarly in mice of both genotypes, subsequent higher doses of leptin yielded further decreases in food intake in Cre+ but not WT mice (Figure 3E). Administration of PBS to the same mice prior to leptin administration yielded no differences in food intake compared to a control group receiving no treatment, while WT mice did show a reduction in food intake (Figures S2A–S2D). This argues against a Cre+-dependent differential response to the stress of the injection.

These results show that in comparison with WT mice, Cre+ mice have increased leptin sensitivity after brief as well as long-term HFD feeding. While studies have shown both beneficial and detrimental consequences of partial leptin levels on diet-induced obesity (Begriche et al., 2008; Asai et al., 2020), a recent report showed that global as well as adipocyte-specific loss of one allele of leptin gene resulted in decreased weight gain upon HFD feeding (Zhao et al., 2020). We wanted to check if leptin levels are affected before subjecting the mice to metabolic stress. We found that Cre+ mice have lower serum leptin levels compared to the WT mice (Figure 3F). We hypothesize that this partial leptin reduction in Cre+ mice may contribute to the observed increase in leptin sensitivity and associated reduction in weight gain. Overall, these results suggest that insertion of the E2a-Cre transgene in the *Obrq2* locus on chromosome 6 reduces baseline circulating leptin levels, increases exogenous leptin sensitivity, protects mice from HFD-induced leptin resistance, and opposes HFD-induced obesity.

Loss of allograft inflammatory factor-1-like (AIF1L) in Cre+ mice reduces circulating leptin levels after short-term HFD feeding

We previously reported that loss of AIF1L reduces *leptin* transcripts in adipose tissues and levels of leptin in circulation (Parikh et al., 2020). Intriguingly, studies of Cre+ mice showed increased AIF1L expression in epididymal white adipose tissue (eWAT) (Figure 4A). These results, along with the observed regulation of leptin in the Cre+ model, led us to evaluate a potential role for AIF1L in this context. To test possible interactions between AIF1L and the Cre+ model, we generated *Aif1l*^{flox};Cre+ mice that are deficient in AIF1L while also bearing the Cre transgene. First, we checked leptin levels at baseline in adult mice and found no difference between Cre+ and *Aif1l*^{flox};Cre+ mice (Figure 4B). We then stressed the mice by subjecting them to HFD feeding for 2 weeks and found that *Aif1l*^{flox};Cre+ mice have lower levels of circulating leptin compared to Cre+ mice (Figure 4B). We further measured fat mass for a subset of this cohort (Figure S3A) and plotted leptin as a function of fat mass, which showed no differences between Cre+ and *Aif1l*^{flox};Cre+ genotypes, indicating that lower leptin levels are not due to lower fat mass (Figure S3B). Given this observed partial reduction in leptin levels in *Aif1l*^{flox};Cre+ mice, we utilized a separate cohort of *Aif1l*^{flox};Cre+ mice fed with HFD for 2 weeks to check leptin sensitivity relative to the WT and Cre+ HFD-fed mice, as reported in Figure 3. Like Cre+ mice, *Aif1l*^{flox};Cre+ mice showed a reduction in food intake in response to exogenous leptin when compared to WT mice intake (Figure 4C); however, we did not observe any further reduction in food intake when compared to the Cre+ mice. This result suggests that the observed increase in leptin sensitivity due to insertion of the E2a-Cre transgene in the *Obrq2* locus is maintained in *Aif1l*^{flox};Cre+ mice. Overall, these results show that when the *Obrq2* QTL is mutated by transgene integration, AIF1L does not affect leptin levels at baseline but is required to maintain leptin levels after short-term HFD feeding.

Loss of AIF1L reverses the obesity resistance of Cre+ mice

Considering that AIF1L-deficient mice have lower levels of circulating leptin than WT mice and maintain greater leptin sensitivity after brief HFD feeding, we wondered if loss of AIF1L would also affect long-term resistance of Cre+ mice to HFD-induced weight gain. To test this idea, we subjected 8- to 9.5-week-old *Aif1l*^{flox};Cre+ mice to HFD feeding for 16 weeks. Remarkably, we found that *Aif1l*^{flox};Cre+ mice displayed accelerated weight gain compared to the Cre+ mice (Figure 5A). Body composition analysis

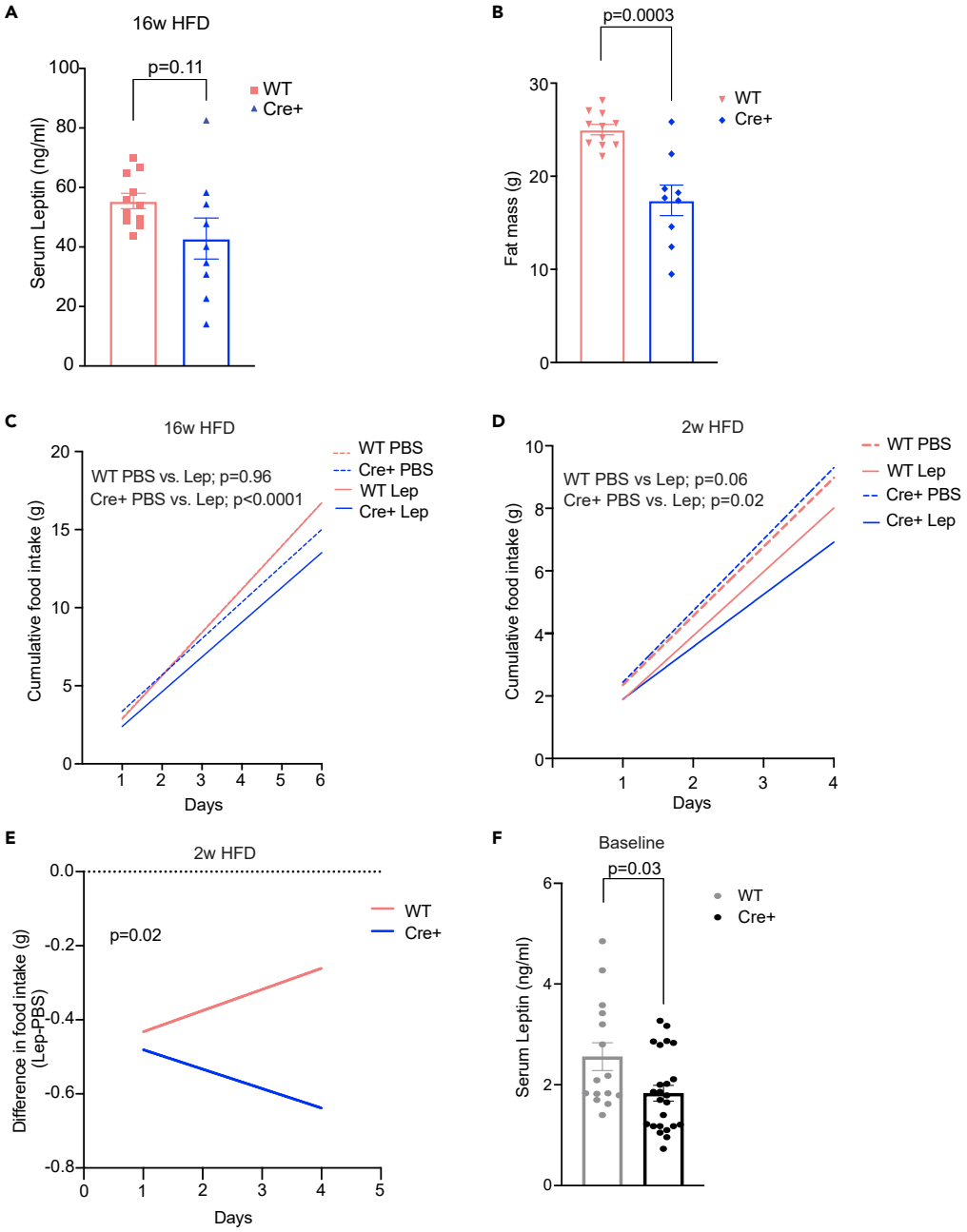

Figure 3. Cre+ mice on HFD show higher responsiveness to exogenous leptin

(A) Circulating leptin levels in serum from 16 weeks HFD-fed WT (n = 11) and Cre+ (n = 9) male mice.

(B) Fat mass of WT (n = 11) and Cre+ (n = 9) male mice after 16 weeks of HFD feeding (a subset of this cohort is also a part of Figure 1C).

(C) Cumulative food intake of single housed 16 weeks HFD-fed male mice measured every 24 h in response to daily PBS or leptin administration (WT; n = 6) (Cre+; n = 4).

(D) Cumulative food intake of single housed 2 weeks HFD-fed male mice measured every 24 h in response to daily PBS or leptin administration (WT; n = 7) (Cre+; n = 4).

(E) Difference in food intake; food intake after leptin administration minus food intake after PBS administration (leptin-PBS) (WT; n = 7) (Cre+; n = 4).

(F) Circulating leptin levels in serum from adult WT (n = 15) and Cre+ (n = 24) male mice at baseline on normal diet. Data are represented as mean ± SEM. See also Figures S1 and S2.

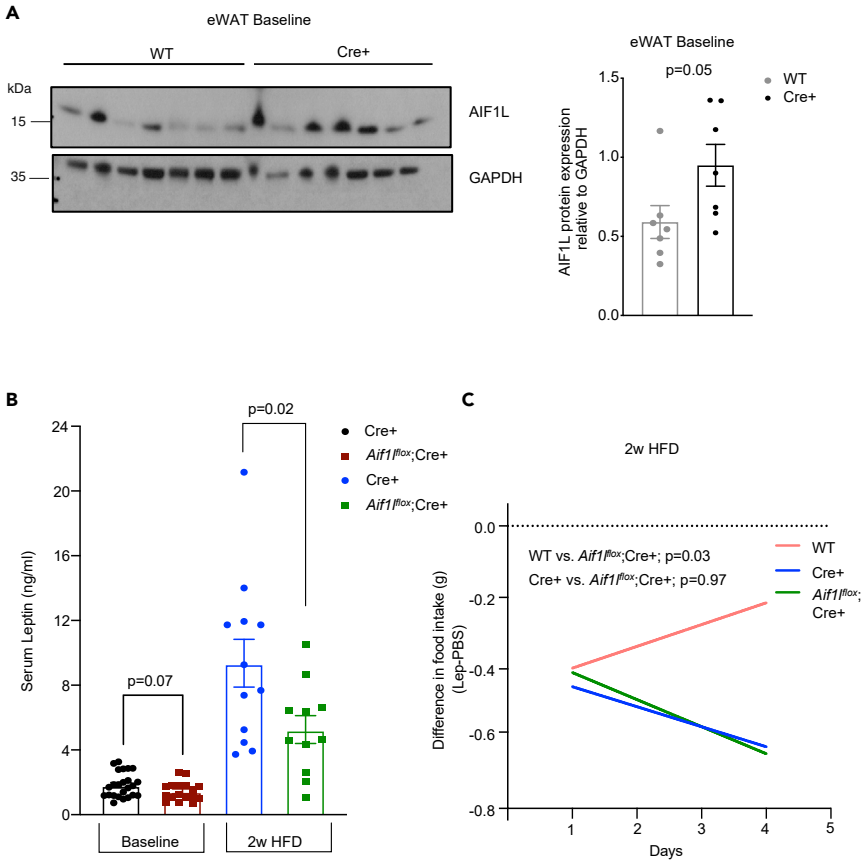

Figure 4. Concurrent loss of allograft inflammatory factor-1-like (AIF1L) in Cre+ mice reduces circulating leptin levels after short-term HFD feeding

(A) AIF1L protein expression in eWAT using immunoblotting in 8–9.5 weeks old WT and Cre+ mice, at baseline on normal diet (n = 7).

(B) Circulating leptin levels in serum from adult Cre+ (n = 24) and *Aif1l*^{flox};Cre+ (n = 17) male mice at baseline (Repetition of Cre+ mice data from Figure 3F, for a new comparison) and 2 weeks HFD-fed Cre+ (n = 12) and *Aif1l*^{flox};Cre+ (n = 11) male mice.

(C) Difference in food intake; food intake after leptin administration minus food intake after PBS administration (leptin-PBS) (*Aif1l*^{flox};Cre+; n = 5) (Repetition of WT and Cre+ mice data from Figure 3E, for a new comparison). Data are represented as mean ± SEM. See also Figures S1 and S3.

revealed that increases in both fat mass as well as lean mass contributed to the increased body weight (Figure 5B), and micro-computerized tomography (μCT) scans yielded similar results (Figure 5C). Additionally, we harvested organs at the end of the study and found that *Aif1l*^{flox};Cre+ mice have increased iSAT and liver mass relative to the Cre+ mice (Figure 5D). Representative macroscopic and histologic appearance of the adipose depots and liver are depicted in Figures S4A and S4B, respectively. These findings show an unexpected reversal of the Cre+ phenotype by loss of AIF1L and suggest a genetic interaction between the *Obrq2* locus—as affected by the transgene insertion—and *Aif1l*.

To assess a possible sexual dimorphic role for this genetic interaction, we also subjected female mice to long-term HFD feeding. We found that female *Aif1l*^{flox};Cre+ mice, like male *Aif1l*^{flox};Cre+ mice, have increased body weight, but with different kinetics—whereas male *Aif1l*^{flox};Cre+ were significantly heavier by 6 weeks of HFD, in females, the weight curves did not diverge until 16 weeks of HFD feeding (Figure 5E). We also observed an increase in fat mass, but no difference in lean mass (Figure 5F). μCT scans also showed that 18 weeks of HFD caused greater fat accumulation in female *Aif1l*^{flox};Cre+ mice compared to Cre+ mice (Figure 5G). We then harvested the organs and found increases in the mass of iSAT, peri-ovarian white adipose tissue (poWAT), and livers from *Aif1l*^{flox};Cre+ mice compared to Cre+ mice (Figure 5H). These results indicate that loss of AIF1L fully suppresses the obesity resistance phenotype of the transgenic mice in both

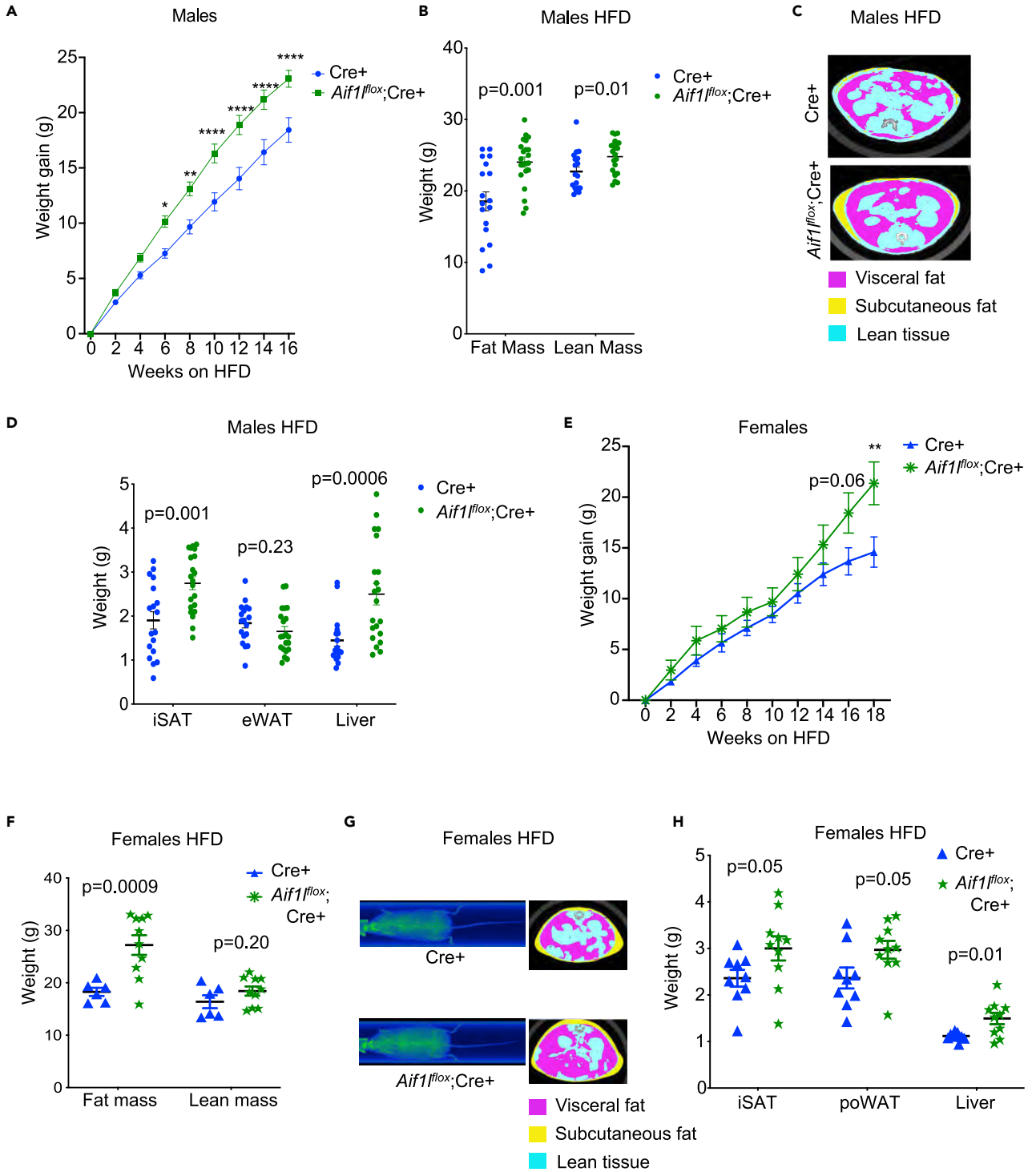

Figure 5. Loss of AIF1L reverses obesity resistance of E2a-Cre transgenic mice

(A) Weight gain curves of Cre+ (n = 26) and *Aif1l*^{flox};Cre+ (n = 28) male mice over 16 weeks of HFD feeding (Cre+ data from Figure 1C is repeated here for a new comparison).

(B) Fat mass and lean mass measurements of 16 weeks HFD-fed male mice, analyzed by Echo MRI (*Aif1l*^{flox};Cre++; n = 18) (*Aif1l*^{flox};Cre+; n = 22) (Cre+ data from Figure 1E is repeated here for a new comparison).

(C) Representative μCT sections of HFD-fed Cre+ and *Aif1l*^{flox};Cre+ male mice.

Figure 5. *Continued*

(D) iSAT, eWAT, and liver mass from 16 weeks HFD-fed male mice (Cre+; n = 18) (*Aif1l*^{flox};Cre+; n = 22) (Cre+ data from Figure 1F is repeated here for a new comparison).

(E) Weight gain curves of Cre+ (n = 9) and *Aif1l*^{flox};Cre+ (n = 10) female mice over 18 weeks of HFD feeding.

(F) Fat and lean mass measurements of 18 weeks HFD-fed female mice, analyzed by Echo MRI (Cre+; n = 6) (*Aif1l*^{flox};Cre+; n = 10).

(G) Representative μCT sections of 18 weeks HFD-fed Cre+ and *Aif1l*^{flox};Cre+ female mice.

(H) iSAT, periovarian white adipose tissue (poWAT), and liver mass from 18 weeks HFD-fed female mice (Cre+; n = 9) (*Aif1l*^{flox};Cre+; n = 10). Data are represented as mean ± SEM. See also Figures S4–S6.

sexes. Also, these results further provide evidence for a genetic interaction between the transgene integration region on chromosome 6 and the *Aif1l* locus on chromosome 2. Overall, we demonstrate that AIF1L limits HFD-induced weight gain when the *Obrq2* obesity QTL is altered.

Loss of AIF1L does not alter energy expenditure, substrate utilization, or glucose tolerance of the HFD-fed Cre+ transgenic mice

We next asked how the loss of AIF1L leads to weight gain in the Cre+ mice fed an HFD. Metabolic cage analyses of mice fed an HFD for 16 weeks showed no difference in energy expenditure between Cre+ and *Aif1l*^{flox};Cre+ mice (Figure S5A). We then wondered if differences in energy expenditure—or other metabolic parameters—early in HFD feeding could explain the phenotype. To test this idea, we performed metabolic cage studies after 1 week of HFD feeding and found no differences in energy expenditure (Figure S5B), physical activity (Figure S5C), or substrate utilization preferences (Figure S5D) between the Cre+ and *Aif1l*^{flox};Cre+ mice. In addition, body length was not different (Figure S5E), which argues against an effect on overall growth as an explanation for differences in body weight. We further assessed glucose tolerance in adult Cre+ and *Aif1l*^{flox};Cre+ mice at baseline and after short-term HFD feeding, and found no differences in fasting glucose levels (Figures S6A and S6D), individual glucose measurements with GTT (Figures S6B and S6E), and mean area under the curve (AUC) quantification (Figures S6C and S6F). These results indicate that AIF1L is not required to maintain basal glucose sensitivity of the transgenic mice, and more importantly, that alterations in glucose sensitivity do not precede weight gain differences upon HFD feeding. Altogether, the absence of significant differences in energy expenditure, substrate utilization, and glucose tolerance between Cre+ and *Aif1l*^{flox};Cre+ mice suggested that food intake differences might underlie the observation that AIF1L limits weight gain by Cre+ mice on an HFD.

Differences in weight gain due to loss of AIF1L depend on food intake

To assess whether AIF1L affects food intake of the Cre+ mice on HFD (Figure 1D), we evaluated this parameter in singly housed *Aif1l*^{flox};Cre+ mice. We observed that cumulative HFD intake of *Aif1l*^{flox};Cre+ mice was significantly higher compared to that of Cre+ mice (Figure 6A), indicating that loss of AIF1L restores food intake of Cre+ mice to WT levels. To corroborate unequivocally whether AIF1L plays a role in regulating energy intake in the Cre+ mice, we performed pair-feeding studies. Adult Cre+ and *Aif1l*^{flox};Cre+ male mice were first socially housed and fed an HFD *ad libitum* for 3 weeks, which resulted in body weight increases for the *Aif1l*^{flox};Cre+ mice relative to Cre+ mice (Figure 6B). For the following 8 weeks, the mice were switched to single housing. The Cre+ mice were fed *ad libitum*, and the *Aif1l*^{flox};Cre+ mice were fed the amount of food eaten by the Cre+ mice the previous day. This pair feeding of the *Aif1l*^{flox};Cre+ mice resulted in normalization of the weight gain differences (Figures 6B and 6C). Subsequently, both groups of mice were socially housed and fed *ad libitum* for 13 weeks (Figure S7A). At the end of the study, we observed increased body weight of *Aif1l*^{flox};Cre+ mice relative to Cre+ mice. Body composition analysis revealed that this increased body weight was due to increased fat mass (Figure S7B). Direct measurements of organs harvested from *Aif1l*^{flox};Cre+ and Cre+ mice showed an increase in mass of iSAT from *Aif1l*^{flox};Cre+ mice (Figure S7C). In combination, these results confirm that energy intake differences drive the weight gain and fat mass differences of the Cre+ and *Aif1l*^{flox};Cre+ mice upon HFD feeding. At the same time, these results indicate that AIF1L prevents HFD-induced weight gain of the Cre+ mice by limiting food intake. Overall, our data reveal an unexpected regulatory function for AIF1L in the context of diet-induced hyperphagia and associated weight gain.

DISCUSSION

With these studies, we have uncovered a previously unknown role for AIF1L in metabolism—specifically, showing that in some settings AIF1L can limit HFD-induced obesity by suppressing food intake. We identified this function in a transgenic mouse line—the E2a-Cre transgenic (Cre+) mouse model—that

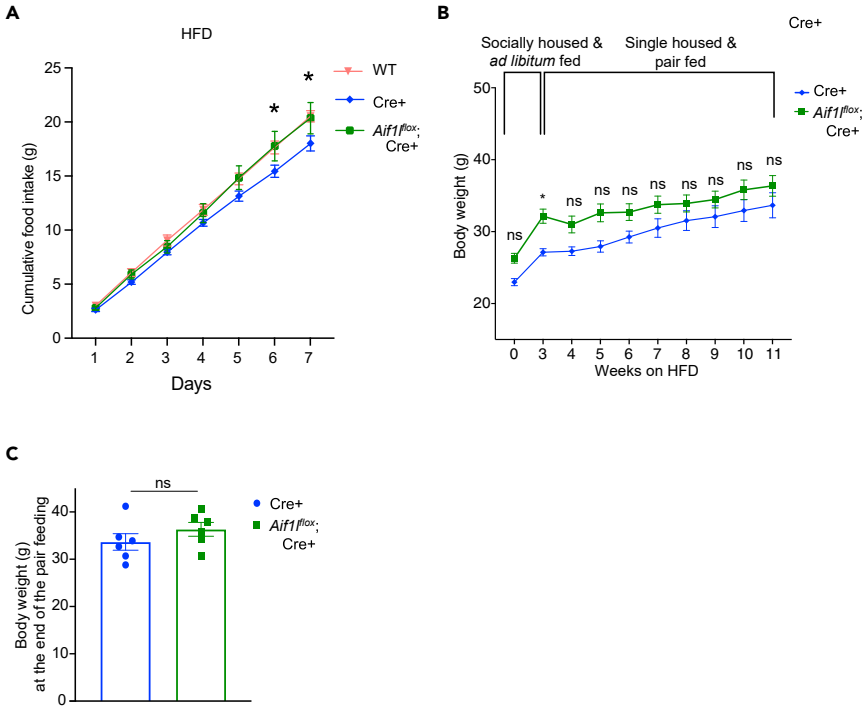

Figure 6. Differences in weight gain due to loss of AIF1L depend on food intake

(A) Cumulative food intake of single housed HFD-fed WT (n = 6), Cre+ (n = 4), and *Aif1l*^{flox};Cre+ (n = 4) male mice measured every 24 h for 7 days (WT and Cre+ data from Figure 1D are repeated here for a new comparison).

(B) Body weight curves of Cre+ and *Aif1l*^{flox};Cre+ male mice over 3 weeks of *ad libitum* HFD feeding followed by 8 weeks of pairwise feeding (n = 6).

(C) Body weight of Cre+ and *Aif1l*^{flox};Cre+ male mice at the end of the pair-feeding study (n = 6). Data are represented as mean ± SEM. See also Figure S7.

displayed limited food intake and decreased weight gain upon HFD feeding. Concurrent loss of AIF1L fully suppressed these phenotypes in both male and female (*Aif1l*^{flox};Cre+) mice. Moreover, we found that pair feeding of *Aif1l*^{flox};Cre+ mice (*i.e.*, limiting intake to that of Cre+ mice) normalized the weight gain differences. These findings support the idea that the AIF1L-dependent obesity phenotype is driven by differences in energy intake. This is the first report showing AIF1L as a context-dependent regulator of HFD-induced hyperphagia and obesity.

We localized the integration site of the widely used E2a-Cre transgene to the *Obrq2* QTL on chromosome 6. This QTL was recognized using chromosome substitution strains (CSS) combining the obesity-susceptible C57BL/6 and obesity-resistant A/J strains. The *Obrq2* QTL was mapped to a 30.3 Mb interval between the SNP markers *rs13478633* and *rs30218447* (Yazbek et al., 2011), an interval that includes the *leptin* gene. Here, we show for the first time that modification of this chromosomal region—as by transgene integration—is associated with reduction of circulating leptin levels in adult mice. We previously reported that AIF1L is expressed in adipose depots and that global loss of function in mice reduces both baseline levels of *leptin* transcripts and levels of leptin in circulation (Parikh et al., 2020). Interestingly, here we observed that brief HFD feeding reduced leptin levels in *Aif1l*^{flox};Cre+ mice relative to Cre+ mice. These results, combined with the reversal of obesity resistance in Cre+ mice due to loss of AIF1L, indicate a genetic interaction between the transgene integration region on chromosome 6 and the *Aif1l* locus on chromosome 2, and suggest that AIF1L acts in the context of HFD feeding as a modifier of the *Obrq2* QTL and leptin levels. While it has been shown that the magnitude of the effect of the *Obrq2* QTL is highly dependent on neighboring QTLs on the same chromosome (Shao et al., 2008; Riordan and Nadeau, 2017), to our knowledge, other single locus modifiers of this QTL have not been identified, making *Aif1l* the first such candidate.

A recent study shows that partial leptin deficiency in adult mice limits HFD-induced weight gain (Zhao et al., 2020); this effect has been explained as protection from hyperleptinemia, which in turn maintains sensitivity to leptin.

Furthermore, partially reducing the leptin levels in the settings of hyperleptinemia, like in obese mice, reverses leptin resistance (Zhao et al., 2019). While the understanding of causes and consequences of hyperleptinemia and complete leptin deficiency has significantly improved due to numerous studies with rodents and humans, the physiology and pathophysiology of partial leptin deficiency is just beginning to emerge. In contrast to these studies that elucidated beneficial effects, detrimental effects of partial leptin deficiency have also been reported in mice as well as humans (Farooqi et al., 2001; Begriche et al., 2008; Asai et al., 2020). In view of these disparate findings, a consensus on the definition of partial/low/extremely low levels of leptin levels is also pending, and critically important to help understand and possibly resolve these conflicting results. Here, we show that the partial leptin reduction in adult Cre+ mice on normal diet is associated with higher leptin sensitivity and decreases in food intake, fat mass, and weight gain. With HFD feeding and coincident loss of AIF1L, however, reduction in leptin levels (by ~45%) is associated with increases in food intake, fat mass, and weight gain, thereby suppressing the metabolic phenotype observed in the Cre+ mice. Further studies will be required to test whether the observed increased leptin sensitivity in Cre+ mice after short-term HFD feeding is due to preexisting partial deficiency of leptin and/or a direct effect independent of the levels. More importantly though, our study particularly highlights the role of AIF1L, which shows modest effects on leptin levels but significant effects on HFD-induced hyperphagia and weight gain.

It is now well established that obesity and its associated metabolic disorders are rarely monogenic; their polygenic and epigenetic nature point to the value of identifying new and different kinds of mouse models to study the underlying complex pathophysiology valuable. The data we report here provide a strong rationale to study the genetic interaction between *Obrq2* and AIF1L in a more physiological model. Buchner et al. have established congenic and sub-congenic strains for this QTL and sub-QTLs on chromosome 6 (Yazbek et al., 2011). Similar strains—wherein these regions of chromosome 6 are perturbed in a controlled fashion—and mouse models with increased leptin sensitivity could be used toward these goals. In addition, these models would make it feasible to study loss of AIF1L in a temporally and adipocyte-restricted context, which is impossible in this transgenic model as the E2a-Cre promoter is active as early as the zygotic stage. We also hypothesize that this interaction is bidirectional in nature, as we observe increase in expression of AIF1L in the eWAT depot from adult Cre+ mice, compared to age-matched WT mice (Figure 4A). This is especially interesting, as we did not observe a similar difference in the iSAT depot. These data provide a rationale for testing AIF1L expression in these depots from HFD-fed mice and studying white adipocyte-specific loss of AIF1L. Further studies are required to check if AIF1L is differentially expressed in other metabolic organs.

In previous studies, we found that global loss of AIF1L did not affect weight gain, fat and lean mass, or metabolic profile in mice on HFD, and we concluded from these observations that AIF1L is not essential for HFD-induced obesity. We also showed that AIF1L is expressed in adipose tissues, brain, and kidney of adult mice (Parikh et al., 2020). The data we report here—uncovered due to the incidental integration of a transgene in chromosome 6—show that AIF1L can indeed play a role in HFD-induced weight gain. These findings provide some new understanding for this little-studied protein. In conclusion, we report that AIF1L limits high-fat diet-induced hyperphagia and weight gain, in the settings of increased leptin sensitivity, potentially through regulating leptin levels.

Limitations of the study

Some caveats for this work should be considered. For one, we have identified a genetic interaction of the *Aif1L* and the *Obrq2* loci through an artificial event—mutation of the *Obrq2* locus induced by integration of an engineered transgene. We are curious to know if the genetic interaction also occurs under different and potentially more physiologic metabolic stressors. We also recognize that the observed diet-induced weight gain phenotypes in our mouse models may be leptin independent, and note that other candidate genes within the *Obrq2* QTL interval remain to be investigated. The nearest coding region to the transgene integration site on chromosome 6 is the gene *Grm8*, which encodes metabotropic glutamate receptor 8. In the context of DIO, variant *rs2237781* within *GRM8* has been suggested to influence eating behavior in humans, potentially through pathways involved in addictive behavior (Gast et al., 2013). Further studies are warranted to investigate the contributions of this and other potential candidate genes in *Obrq2* interval, and their interaction with *Aif1l* in regulating the observed fat mass phenotype.

STAR★METHODS

Detailed methods are provided in the online version of this paper and include the following:

SUPPLEMENTAL INFORMATION

Supplemental information can be found online at https://doi.org/10.1016/j.isci.2022.105058.

ACKNOWLEDGMENTS

Supported by NIH R01HL128066, R21NS16480, and R21AI171739 (N.E.S.S.), F31HL144041 and T32 GM007491 (V.A.), American Heart Association 20TPA35490392 (N.E.S.S.) and Career Development Award 19CDA34660217 (D.F.R-B.). We would like to thank Cergentis BV (Utrecht, the Netherlands) for performing the TLA and sequencing. We would like to thank Gary Schwartz (Einstein) for key advice and the Einstein Diabetes Center Animal Physiology core facility for assistance with performing Echo-MRI, CT scans, and metabolic cage studies. We would also like to thank the histopathology core facility and biomarker analytic research core (BARC) Einstein for help with H&E staining and serum analyte measurements, respectively. We would also like to acknowledge that the graphical abstract was created with biorender.com.

AUTHOR CONTRIBUTIONS

Conception and design N.E.S.S., D.P.; Performance of experiments D.P., D.F.R-B., S.J., G.O-P., V.A.; Analysis of data D.P., D.F.R-B., N.E.S.S.; Figures and writing D.P., N.E.S.S.

DECLARATION OF INTERESTS

The author(s) declare no competing interests.

Received: March 29, 2022
Revised: July 28, 2022
Accepted: August 29, 2022
Published: October 21, 2022

REFERENCES

Anderson, M.R., Geleris, J., Anderson, D.R., Zucker, J., Nobel, Y.R., Freedberg, D., Small-Saunders, J., Rajagopalan, K.N., Greendyk, R., Chae, S.R., et al. (2020). Body mass index and risk for intubation or death in SARS-CoV-2 infection : a retrospective cohort study. Ann. Intern. Med. *173*, 782–790. https://doi.org/10.7326/M20-3214.

Asai, A., Nagao, M., Hayakawa, K., Miyazawa, T., Sugihara, H., and Oikawa, S. (2020). Leptin production capacity determines food intake and susceptibility to obesity-induced diabetes in Oikawa–Nagao Diabetes-Prone and Diabetes-Resistant mice. Diabetologia *63*, 1836–1846. https://doi.org/10.1007/s00125-020-05191-8.

Begriche, K., Lettéron, P., Abbey-Toby, A., Vadrot, N., Robin, M.A., Bado, A., Pessayre, D., and Fromenty, B. (2008). Partial leptin deficiency favors diet-induced obesity and related metabolic disorders in mice. Am. J. Physiol. Endocrinol. Metab. *294*, 939–951. https://doi.org/10.1152/ajpendo.00379.2007.

Buchner, D.A., Burrage, L.C., Hill, A.E., Yazbek, S.N., O'Brien, W.E., Croniger, C.M., and Nadeau, J.H. (2008). Resistance to diet-induced obesity in mice with a single substituted chromosome. Physiol. Genomics *35*, 116–122. https://doi.org/10.1152/physiolgenomics.00033.2008.

Buchner, D.A., Geisinger, J.M., Glazebrook, P.A., Morgan, M.G., Spiezio, S.H., Kaiyala, K.J., Schwartz, M.W., Sakurai, T., Furley, A.J., Kunze, D.L., et al. (2012). The juxtaparanodal proteins CNTNAP2 and TAG1 regulate diet-induced obesity. Mamm. Genome *23*, 431–442. https://doi.org/10.1007/s00335-012-9400-8.

Colditz, G.A., and Peterson, L.L. (2018). Obesity and cancer: evidence, impact, and future directions. Clin. Chem. *64*, 154–162. https://doi.org/10.1373/clinchem.2017.277376.

de Vree, P.J.P., de Wit, E., Yilmaz, M., van de Heijning, M., Klous, P., Verstegen, M.J.A.M., Wan, Y., Teunissen, H., Krijger, P.H.L., Geeven, G., et al. (2014). Targeted sequencing by proximity ligation for comprehensive variant detection and local haplotyping. Nat. Biotechnol. *32*, 1019–1025. https://doi.org/10.1038/NBT.2959.

Farooqi, I.S., Jebb, S.A., Langmack, G., Lawrence, E., Cheetham, C.H., Prentice, A.M., Hughes, I.A., McCamish, M.A., and O'Rahilly, S. (1999). Effects of recombinant leptin therapy in a child with congenital leptin deficiency. N. Engl. J. Med. *341*, 879–884. https://doi.org/10.1056/nejm199909163411204.

Farooqi, I.S., Keogh, J.M., Kamath, S., Jones, S., Gibson, W.T., Trussell, R., Jebb, S.A., Lip, G.Y., and O'Rahilly, S. (2001). Metabolism: partial leptin deficiency and human adiposity. Nature *414*, 34–35. https://doi.org/10.1038/35102112.

Gast, M.T., Tönjes, A., Keller, M., Horstmann, A., Steinle, N., Scholz, M., Müller, I., Villringer, A., Stumvoll, M., Kovacs, P., and Böttcher, Y. (2013). The role of rs2237781 within GRM8 in eating behavior. Brain Behav. *3*, 495–502. https://doi.org/10.1002/brb3.151.

Gruzdeva, O., Borodkina, D., Uchasova, E., Dyleva, Y., and Barbarash, O. (2019). Leptin resistance: underlying mechanisms and diagnosis. Diabetes Metab. Syndr. Obes. *12*, 191–198. https://doi.org/10.2147/DMSO.S182406.

Hubert, H.B., Feinleib, M., McNamara, P.M., and Castelli, W.P. (1983). Obesity as an independent risk factor for cardiovascular disease: a 26- year follow-up of participants in the Framingham Heart Study. Circulation *67*, 968–977. https://doi.org/10.1161/01.CIR.67.5.968.

Knight, Z.A., Hannan, K.S., Greenberg, M.L., and Friedman, J.M. (2010). Hyperleptinemia is required for the development of leptin resistance. PLoS One *5*. e11376–8. https://doi.org/10.1371/journal.pone.0011376.

Kompaniyets, L., Goodman, A.B., Belay, B., Freedman, D.S., Sucosky, M.S., Lange, S.J., Gundlapalli, A.V., Boehmer, T.K., and Blanck, H.M. (2021). Body mass index and risk for COVID-19–related hospitalization, intensive Care unit admission, invasive mechanical ventilation, and death — United States, march–december 2020. MMWR Morb. Mortal. Wkly. Rep. *70*, 355–361. https://doi.org/10.15585/mmwr.mm7010e4.

Kuehn, B.M. (2021). More severe obesity leads to more severe COVID-19 in study. JAMA *325*, 1603. https://doi.org/10.1001/jama.2021.4853.

Lakso, M., Pichel, J.G., Gorman, J.R., Sauer, B., Okamoto, Y., Lee, E., Alt, F.W., and Westphal, H. (1996). Efficient in vivo manipulation of mouse genomic sequences at the zygote stage. Proc. Natl. Acad. Sci. USA *93*, 5860–5865. https://doi.org/10.1073/pnas.93.12.5860.

Li, H., and Durbin, R. (2010). Fast and accurate long-read alignment with Burrows–Wheeler transform. Bioinformatics *26*, 589–595. https://doi.org/10.1093/BIOINFORMATICS/BTP698.

Li, W.D., Li, D., Wang, S., Zhang, S., Zhao, H., and Price, R.A. (2003). Linkage and linkage disequilibrium mapping of genes influencing human obesity in chromosome region 7q22.1-7q35. Diabetes *52*, 1557–1561. https://doi.org/10.2337/diabetes.52.6.1557.

Li, L., Liu, D.W., Yan, H.Y., Wang, Z.Y., Zhao, S.H., and Wang, B. (2016). Obesity is an independent risk factor for non-alcoholic fatty liver disease: evidence from a meta-analysis of 21 cohort studies. Obes. Rev. *17*, 510–519. https://doi.org/10.1111/obr.12407.

Montague, C.T., Farooqi, I.S., Whitehead, J.P., Soos, M.A., Rau, H., Wareham, N.J., Sewter, C.P., Digby, J.E., Mohammed, S.N., Hurst, J.A., et al. (1997). Congenital leptin deficiency is associated with severe early-onset obesity in humans. Nature *387*, 903–908. https://doi.org/10.1038/43185.

Ogus, S., Ke, Y., Qiu, J., Wang, B., and Chehab, F.F. (2003). Hyperleptinemia precipitates diet-induced obesity in transgenic mice overexpressing leptin. Endocrinology *144*, 2865–2869. https://doi.org/10.1210/en.2002-0178.

Parikh, D., Riascos-Bernal, D.F., Egaña-Gorroño, L., Jayakumar, S., Almonte, V., Chinnasamy, P., and Sibinga, N.E.S. (2020). Allograft inflammatory factor-1-like is not essential for age dependent weight gain or HFD-induced obesity and glucose insensitivity. Sci. Rep. *10*, 3594. https://doi.org/10.1038/s41598-020-60433-4.

Pelleymounter, M.A., Cullen, M.J., Baker, M.B., Hecht, R., Winters, D., Boone, T., and Collins, F. (1995). Effects of the obese gene product on body weight regulation in ob/ob mice. Science *269*, 540–543. https://doi.org/10.1126/science.7624776.

Riordan, J.D., and Nadeau, J.H. (2017). From peas to disease: modifier genes, network resilience, and the genetics of health. Am. J. Hum. Genet. *101*, 177–191. https://doi.org/10.1016/j.ajhg.2017.06.004.

Shao, H., Burrage, L.C., Sinasac, D.S., Hill, A.E., Ernest, S.R., O'Brien, W., Courtland, H.W., Jepsen, K.J., Kirby, A., Kulbokas, E.J., et al. (2008). Genetic architecture of complex traits: large phenotypic effects and pervasive epistasis. Proc. Natl. Acad. Sci. USA *105*, 19910–19914. https://doi.org/10.1073/pnas.0810388105.

Tartof, S.Y., Qian, L., Hong, V., Wei, R., Nadjafi, R.F., Fischer, H., Li, Z., Shaw, S.F., Caparosa, S.L., Nau, C.L., et al. (2020). Obesity and mortality among patients diagnosed with COVID-19: results from an integrated health Care organization. Ann. Intern. Med. *173*, 773–781. https://doi.org/10.7326/M20-3742.

Yazbek, S.N., Spiezio, S.H., Nadeau, J.H., and Buchner, D.A. (2010). Ancestral paternal genotype controls body weight and food intake for multiple generations. Hum. Mol. Genet. *19*, 4134–4144. https://doi.org/10.1093/hmg/ddq332.

Yazbek, S.N., Buchner, D.A., Geisinger, J.M., Burrage, L.C., Spiezio, S.H., Zentner, G.E., Hsieh, C.W., Scacheri, P.C., Croniger, C.M., and Nadeau, J.H. (2011). Deep congenic analysis identifies many strong, context-dependent QTLs, one of which, Slc35b4, regulates obesity and glucose homeostasis. Genome Res. *21*, 1065–1073. https://doi.org/10.1101/gr.120741.111.

Zhao, S., Zhu, Y., Schultz, R.D., Li, N., He, Z., Zhang, Z., Caron, A., Zhu, Q., Sun, K., Xiong, W., et al. (2019). Partial leptin reduction as an insulin sensitization and weight loss strategy. Cell Metab. *30*, 706–719.e6. https://doi.org/10.1016/j.cmet.2019.08.005.

Zhao, S., Li, N., Zhu, Y., Straub, L., Zhang, Z., Wang, M.Y., Zhu, Q., Kusminski, C.M., Elmquist, J.K., and Scherer, P.E. (2020). Partial leptin deficiency confers resistance to diet-induced obesity in mice. Mol. Metab. *37*, 100995. https://doi.org/10.1016/j.molmet.2020.100995.

STAR★METHODS

KEY RESOURCES TABLE

REAGENT or RESOURCE	SOURCE	IDENTIFIER
Antibodies		
Rabbit polyclonal anti-GAPDH	Santa Cruz Biotechnology	Cat# sc-25778; RRID: AB_10167668
Rabbit polyclonal anti-AIF1L	Sigma-Aldrich	Cat# HPA020522; RRID: AB_2670463
Chemicals, peptides, and recombinant proteins		
Recombinant Murine leptin	Peprotech	Cat#450–31
Critical commercial assays		
Leptin ELISA kit	Millipore	Cat#EZML-82K
Experimental models: Organisms/strains		
Mouse: E2a-Cre transgenic	Jackson laboratories	Cat#003724
Mouse: *Aif1L* "KO-first" allele on C57BL6/N strain	KOMP/WTSI	#333333; N/A
Oligonucleotides		
Primers for genotyping	Parikh et al., 2020	N/A
Cre primer: for TLA Forward- ATTACGTATATCCTGGCAGC	This paper	N/A
Cre primer: for TLA Reverse- GCCAAGCTATCCCATAAGC	This paper	N/A
Backbone primer for TLA: Forward- GTCCCAACTCACTCTTCTTG	This paper	N/A
Backbone primer for TLA: Reverse- GCCAAGCTATCCCATAAGC	This paper	N/A
Software and algorithms		
ImageJ	National Institutes of Health	https://imagej.nih.gov/ij/
GraphPad Prism 8 and 9	GraphPad	https://www.graphpad.com
Other		
High fat diet; 60% of kCal from fat	Research Diets	Cat#D12492i
Pico Lab mouse diet 20 5058	Lab Diet	Code#5058

RESOURCE AVAILABILITY

Lead contact

Further information and requests for resources and reagents should be directed to and will be fulfilled by the lead contact, Nicholas Sibinga (nicholas.sibinga@einsteinmed.edu).

Materials availability

This study did not generate new unique reagents.

Data and code availability

- Data reported in this paper will be shared by the lead contact upon request.
- This paper does not report original code.
- Any additional information required to reanalyze the data reported in this paper is available from the lead contact upon reasonable request.

EXPERIMENTAL MODEL AND SUBJECT DETAILS

Mouse lines and conditions

Mice bearing the *Aif1L* "KO-first" allele on a C57BL6/N background were obtained from Knockout Mouse Project repository (KOMP). They were backcrossed for 8 generations to the C57BL6/J strain before mating them with E2a-Cre transgenic mice (Jackson laboratories #003724) to generate AIF1L-deficient mice with the *lacZ* gene driven by the endogenous *Aif1l* promoter. Mice were studied between 8 and 24 weeks of age; both male and female mice were evaluated, and results were analyzed and reported separately. All animals were housed in pathogen-free conditions, and procedures were in accordance with the rules and regulations of the Association for Assessment and Accreditation of Laboratory Animal Care (AAALAC) and were approved by the Institutional Animal Care and Use Committee (IACUC) of the Albert Einstein College of Medicine. All the WT and Cre+ mice used for weight gain studies were littermates. One-third of the $Aif1l^{flox}$;Cre+ mice were littermates with WT and Cre+ mice. Breeders of non-littermate cohorts came from the same founder animals. For weight gain studies, strategies used for mating were such that the E2a-Cre transgene was always inherited paternally for all the Cre+ and $Aif1l^{flox}$;Cre+ mice. For baseline and early HFD feeding studies, cohorts of maternally inherited transgenic mice were also included.

METHOD DETAILS

Genotyping

Genotyping was done using genomic DNA extracted from tail tips using tail lysis buffer and proteinase K with overnight digestion at 56°C. Proteinase K was deactivated at 92°C for 20 min and samples were centrifuged to remove the debris. Supernatant was used to perform PCR reactions. Genotyping strategies, primer information, and validation of this mouse line has been reported in our previous study (Parikh et al., 2020).

Diet-induced obese mouse models

Mice aged 8–9.5 weeks were subjected to HFD feeding (Research Diets, D12492i; 60% of kCal from fat) for periods as indicated in the figures. Two independent cohorts were analyzed. The mice were weighed before switching and thereafter every 2 weeks unless otherwise indicated. At the end of the HFD-feeding period, outlier tests were run, and the single outliers (n = 1) identified for each genotype were removed from the analysis. In addition, 1 or 2 mice of each genotype developed skin wounds during the study, and these animals were also removed from the final analysis.

Body composition and imaging

Lean mass and fat mass were acquired using an EchoMRI-100 Body composition analyzer. μCT scan was performed with the following settings – 0.08 mm, 30 slices, and slow speed.

Indirect calorimetry analysis

Columbus Labs comprehensive lab animal monitoring systems (CLAMS, Einstein Animal Physiology Core) were used to collect multiparameter metabolic data, including energy expenditure (EE), physical activity as horizontal and vertical beam breaks, O_2 consumption, and CO_2 production to calculate respiratory exchange ratio (RER). All parameters were normalized to lean mass of each mouse. Data was continuously collected for 5 days after 48h of acclimatization in the cages, in which the mice were individually housed. These assays were done after either 1 week or 16 weeks of HFD feeding, as indicated in the figure legends.

Food intake

HFD-fed male and female mice were single housed and provided *ad libitum* access to food and water. After acclimatization period of 2 days, remaining food was measured every 24h, just before the start of the dark cycle begins (zeitgeber time (ZT) 13.5). The bedding of the cage was checked to account for littering in the food intake analysis.

Pair feeding studies

Male mice aged 8–9.5 weeks were socially housed in groups 2–3 mice per cage and provided *ad libitum* access to food and water for 3 weeks. Thereafter, the mice were switched to single housing. After the acclimatization period of 2 days, food eaten over 24h by each Cre+ mouse was measured. The bedding of the cage was checked for every cage to account for littering.

The following day, *Aif1l*^{flox};Cre+ mice were given the same amount of food eaten by Cre+ mice, and this was repeated daily, for 8 weeks. Subsequently, the mice were again socially housed in the same groups and were provided *ad libitum* access to food and water for 13 weeks. At the end of the study, body composition was measured and adipose tissues, and liver were harvested. In this study, a single mouse was removed after switching to *ad libitum feeding* as it spontaneously developed a white eye.

Leptin sensitivity

Mice representing the mean and range of observed body weight for each genotype were fed an HFD for 16 weeks were switched to single housing and provided *ad libitum* access to food and water. After the acclimatization period and measuring food intake without any injection, PBS was administered intraperitoneally every 24h for indicated days to acclimatize the mice to the stress of the injection before starting leptin administration, and to confirm if the effect seen with leptin is specific or a side effect of the injection itself. Following this PBS administration period, mice were intraperitoneally injected with recombinant leptin (Peprotech, 450–31) with the following regime: 3 μg/g of BW for 2 days followed by 4 μg/g of BW for 2 days followed by 5 μg/g of BW for 2 days. Food intake measurements were done at 4 and 24h after the time of injection. For mice fed HFD for 2 weeks, leptin was injected with the following regime: 1.5 μg/g of BW for 2 days followed by 3 μg/g of BW for 2 days. Leptin or PBS was administered at the same time each day, just before the start of the dark cycle (ZT 13.5).

Circulating leptin measurements

Blood samples were collected from mice at indicated time points without fasting. Serum was prepared by low-speed centrifugation at 4°C. Aliquots were immediately frozen and stored at −80°C until analysis. Leptin levels were measured by ELISA according to manufacturer's instructions (EZML-82K Milipore).

Glucose sensitivity

Fasting blood glucose levels and intraperitoneal GTT were measured in tail blood using a OneTouch Ultra 2 glucometer, after fasting the animals overnight. Animals were challenged with 1 g/kg (according to body weight) of glucose.

Tissue preparation

Mice at different time points, as indicated in figure legends were anesthetized with an intraperitoneal injection of ketamine and xylazine. Organs were isolated and a small piece from each was immediately frozen for RNA and protein isolation. Remaining parts were fixed in 10% formalin for 24h and then transferred to 70% ethanol.

Histological analysis

Tissue samples fixed for 24h were processed and embedded in paraffin at the Einstein Histopathology core facility. They were sectioned at 5 μm and a routine H&E staining was performed.

Immunoblotting

Frozen tissues were homogenized in RIPA lysis buffer (50 mM Tris-HCL pH 7.4, 1% NP40, 0.5% sodium deoxycholate, 0.1% SDS, 1mM EDTA, 150 mM NaCl) with protease inhibitors (Complete, Roche) and phosphatase inhibitors (Roche; PhosSTOP Easypack 04906837001) for protein extraction and then centrifuged to defat and remove debris. Protein concentrations were measured by a BCA protein assay kit (Pierce). Equal amounts of protein (20–60 μg) were loaded, separated by 10–20% Tricine gel (Invitrogen; EC6625BOX) electrophoresis and blotted onto 0.2 μm pore size PVDF membranes (Immobilon-P, Millipore). After blocking in TBST (Tris pH 8.0, NaCl 150 mM, 0.1% Tween 20) plus 5% (w/v) non-fat milk, blots were incubated at 4°C overnight with primary antibodies. Signals were detected with horseradish peroxidase-conjugated secondary antibody and chemiluminescence (ECL blotting substrate, Pierce; 32106). Equivalent protein loading was tested with anti-GAPDH antibody (Santa Cruz, sc-25778, 1:5000 dilution). Primary antibodies used: anti-AIF1L (Atlas antibodies, HPA020522, 1:500 dilution). Densitometric analysis was performed using ImageJ software.

Targeted locus amplification

TLA was performed with frozen mouse splenocytes by Cergentis, Utrecht, Netherlands, to identify the transgene integration site. Viable frozen mouse spleen cells were harvested and provided to Cergentis

and were then processed at their facility according to an established protocol (de Vree et al., 2014). Two primer sets were designed on the transgene. Cre primers: Forward- ATTACGTATATCCTGGCAGC Reverse-GGAGTTTCAATACCGGAGAT. Backbone primers: Forward-GTCCCAACTCACTCTTCTTG. Reverse- GCCAAGCTATCCCATAAGC. The primer sets were used in individual TLA amplifications. PCR products were purified, and a library was prepped using the Illumina Nextera flex protocol and sequenced on an Illumina sequencer. Reads were mapped using BWA-SW (Li and Durbin, 2010), version 0.7.15-r1140, settings bwasw -b 7. The NGS reads were aligned to the Tg sequence and host genome. The mouse mm10 genome was used as host reference genome sequence.

QUANTIFICATION AND STATISTICAL ANALYSIS

Based on results of a pilot study for body weight gain curves on 60% HFD-fed WT mice, we used power analysis to determine the minimum number of mice per group that would be adequate to ensure 80% power to detect 40% change in mean weight gain, assuming a two-sided test and alpha of 0.05. For single time-point measurements, statistical analyses were performed using unpaired t tests with Welch's correction for two groups. For repeated measurements, ANOVA was performed, with Bonferroni's multiple comparison correction tests. AUC was measured for glucose and insulin tolerance tests. Cumulative food intake differences were analyzed using nonlinear regression fit Gaussian model. Cumulative food intake differences without treatment were analyzed using two-way ANOVA with multiple comparison correction tests. Leptin levels as a function of fat mass was analyzed using linear regression. A p value less than 0.05 was considered statistically significant. All analysis was performed using GraphPad Prism 8 and data were expressed as mean $\pm$ SEM.